CHAOTIC LASERS: MANIFOLDS, BIFURCATIONS AND SYMBOLIC DYNAMICS

PIETER COLLINS*
Centrum voor Wiskunde en Informatica
P.O. Box 94079
1090 GB Amsterdam, The Netherlands

BERND KRAUSKOPF†
Department of Engineering Mathematics
University of Bristol
Bristol BS8 1TR, UK

An optically-injected semiconductor laser exhibits chaotic behaviour for certain values of the parameters. The underlying model is an example of a general three-dimensional system of ordinary differential equations, and existing analyses agree very well with experiments. We outline a method for computing an approximate but powerful description of the behaviour in the chaotic regime in terms of symbolic dynamics. The method is based on computing the stable and unstable manifolds of the system, which can then be used to give a natural description of the orbits.

1. Semiconductor laser with optical injection

Understanding the dynamics of laser systems is important in many application areas, such as optical communication through glass fibres, reading of optical disks, and, more speculatively, chaotic communication and chaotic computing. We demonstrate here a method of how chaotic dynamics can be analysed, and for this we use the example of an optically injected single-mode semiconductor laser. This laser system is described well by the rate equations[7]

$$\dot{E} = K + \left(\tfrac{1}{2}\left(1 + i\alpha\right) n - i\omega\right) E$$
$$\dot{n} = -2\Gamma n - \left(1 + 2Bn\right)\left(|E|^2 - 1\right)$$

*work partially supported by Leverhulme Special Research Fellowship SRF/4/9900172.
†work partially supported by an EPSRC Advanced Research Fellowship.

for the complex electric field, $E = E_x + iE_y$, and the population inversion in the laser cavity, n. Further, B, Γ and α are fixed parameters depending on the characteristics of the laser in question; realistic values for a semiconductor laser are $B = 0.015$, $\gamma = 0.035$ and $\alpha = 2.000$ that remain fixed throughout this paper. The injected field rate K and detuning frequency ω are control parameters that can be changed in an experiment.

The injected semiconductor laser provides a realistic example of a fully three-dimensional flow (no symmetries or invariants). Theory suggests that much of the behaviour of low-dimensional systems is determined by the stable and unstable manifolds W^s and W^u of suitable saddle periodic orbits[6]. If P is a saddle periodic orbit and $W^u(P)$ and $W^s(P)$ intersect transversely then they must do so on *infinitely* many orbits, forming a complicated figure called a *tangle*. It is well known that the a system with such a tangle is chaotic. Bifurcations occur when W^u and W^s are tangent. These bifurcations are extremely complicated and can involves large changes (explosions) in the attractors of a system[4].

When one goes from a vector field in three dimensions to a two-dimensional map by considering the Poincaré return map to a section, one generally does not obtain a *global diffeomorphism* of the plane. (The exceptions are periodically forced systems.) This is so because, in general, it is impossible to find a section that is everywhere transverse to the flow of the vector field[8].

Specifically, for the injection laser we consider the section $\Sigma = \{(E, n) : n = 0\}$. On Σ we have $\dot{n} = 1 - |E|^2$, so the flow is tangent to Σ on the circle $C = \{(E, n) : |E| = 1, n = 0\}$. As a result, the first Poincaré return map is *discontinuous* on the circle C. This discontinuity is not an artefact of choosing a 'strange' type of section, and it cannot be removed by a perturbation of the section.

Discontinuous return maps exhibit new phenomena that are not seen in differentiable systems. We remark that similar phenomena also occur naturally in impact oscillators, singular limits, and switched/hybrid systems. A detailed dicussion of the dicontinuities and their bifurcations in general Poincaré maps of vector fields is beyond the scope of this paper and will be reported elsewhere.

However, we remark that stable and unstable manifolds of a discontinuous Poincaré map may consist of different invariant curves and exhibit new phenomena which are not found in systems with a continuous first return map. For example, two points on the same periodic orbit may lie on the same invariant curve, and some invariant curves may not contain

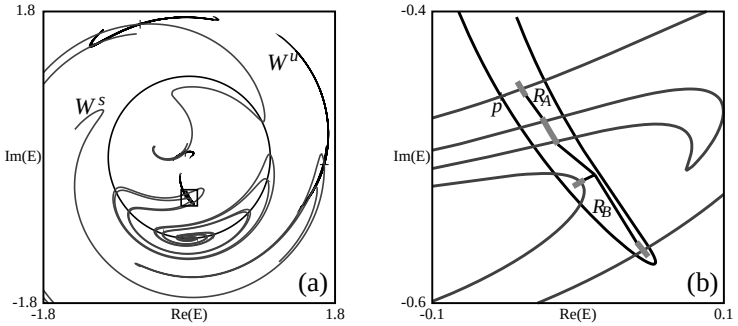

Figure 1. Stable and unstable manifolds of the period-4 orbit P of the first return map to Σ (a), and an enlargemnt showing a trellis with its associated graph; the parameters are $K = 0.290$, $\omega = 0.278$.

any periodic points. Intersecting invariant curves of a tangle need not intersect infinitely many times, and invariant curves may be circles as well as immersed or embedded arcs. These phenomena can all be understood in terms of intersections of two-dimensional invariant manifolds with the two-dimensional Poincaré section.

Figure 1 (a) shows one-dimensional stable and unstable manifolds in the Poincaré section Σ defined above. These manifolds were found by computing the Poincaré return map directly with a shooting method. This method is quite straightforward, but growing the manifolds continuously requires changing the iterate of the return map used to compute (pre)images. However, this is much easier than computing the full two-dimensional manifolds manifold directly[5], and then its intersection with Σ.

2. Symbolic dynamics of the injection laser

Since it is impossible to compute a whole tangle, we restrict attention to finite subsets $T^u \subset W^u$ and $T^s \subset W^s$. The pair $T = (T^u, T^s)$ is called a *trellis*. We write $(f; T)$ if f is a diffeomorphism with a trellis T. Our goal is to compute invariants of the *trellis type* $[f; T]$ which is the isotopy/conjugacy class of $(f; T)$. If the intersections of T^u and T^s are transverse, the topology of T is robust with respect to perturbations. The entropy of a trellis type, denoted $h_{top}[f; T]$, is the *infimum* of the topological entropy of the models of $[f; T]$.

The set of *intersection points* is $T^v = T^u \cap T^s$, and consists of periodic, homoclinic and heteroclinic orbits. A *region* of a trellis is the closure of a component of the complement of $T^u \cup T^s$. A *segment* is an (open) interval

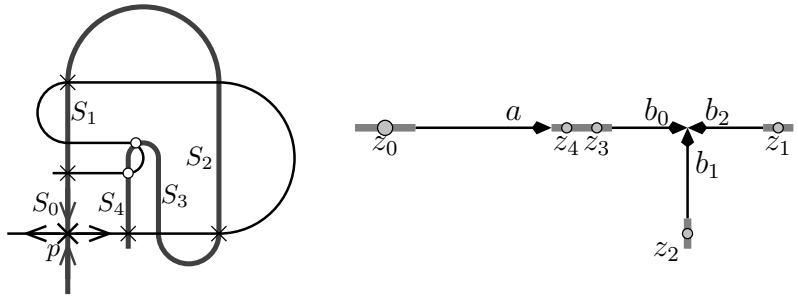

Figure 2. A topological sketch of the trellis in Fig. 1 (b) and its restricted graph representative.

of T^u or T^s with endpoints, but no interior points, in T^v.

The *graph representative* $(g; G, W)$ of $(f; T)$ is a one-dimensional representation of the dynamical and geometrical properties. The graph G is a one-dimensional CW-complex embedded as a deformation retract of $\mathcal{C}T^u$, the complement of T^u, and W is the set of intersections of G with T^s. Each segment of T^s contains exactly one point of W, each edge of G contains at most one point of W, and g is a CW-map of (G, W) which is homotopy-equivalent to f on $\mathcal{C}T^u$. The map g maps the control edge z crossing segment S to the control edge $g(z)$ crossing $f(S)$. The edges of G crossing T^s (i.e. those that contain a point of W) are *control edges*; other edges are *expanding edges*. The map g is locally injective on the expanding edges. For any (irreducible) trellis type, the graph representative is unique, and can be computed using a variant of the Bestvina-Handel algorithm for train-tracks[1]. All the chaotic dynamics is carried by the *restricted graph representative*, which is the restriction of g to $\widetilde{G} = \bigcap_{n=0}^{\infty} g^n(G)$.

An *itinerary* of an orbit is a sequence of regions (R_i) such that $f^i(x) \in R_i$ for all $i \in \mathbf{N}$. The following result shows how to relate the dynamics of the graph representative to that of the trellis type[2].

Theorem 2.1. *Let $(g; G, W)$ be the graph representative of $(f; T)$. Then for every orbit (y_i) of g, there is an orbit (x_i) of f with the same itinerary. Further, if (y_i) is periodic or homoclinic, then the orbit (x_i) can also be taken to be periodic or homoclinic. The topological entropy of g is a lower bound for the topological entropy of f.*

The symbolic dynamics given by g typically represents transient behaviour, but for some trellis configurations it gives information on the dynamics on a *numerically* observed strange attractor.

To use the trellis theory to compute symbolic dynamics in the injection laser, we compute a trellis T for the return map f. The fourth return map to Σ is continuous in the rectangle

$$R = [-0.1, 01] \times [-0.6, -0.4]$$

(shown in Figure 1(a)), leading to the trellis and graph shown in Figure 1(b). We compute symbolic dynamics for orbits that remain in R, giving the itinerary in terms of the indicated regions R_A and R_B.

A schematic diagram of the trellis of Figure 1(b) is shown in Figure 2, together with its restricted graph representative. The action of the graph representative on the control edges can be deduced from the action of the fourth return map on the stable manifold, giving

$$z_0, z_1 \mapsto z_0, \quad z_2 \mapsto z_1, \quad z_3, z_4 \mapsto z_0 \,.$$

The dynamics of the resticted graph representative map g is carried by the expanding edges a, b_0, b_1 and b_2:

$$a \mapsto a\bar{z}_4 z_3 b_1 \bar{b}_2, \quad b_1 \mapsto b_2, \; b_2 \mapsto b_3, \; b_3 \mapsto a\bar{z}_4 z_3 b_1 \,.$$

Therefore, chaotic dynamics must exist in the regions R_A and R_B. All itineraries are forced except for those containing the words $R_A R_B^{3n+1} R_A$ for some $n \in \mathbf{N}$. The topological entropy of the return map is at least 0.5280. By computing a larger trellis, the symbolic dynamics can be refined and the entropy bound increased to 0.654. The accuracy of the entropy bound is limited only by how long the manifolds can be computed accurately.

Varying parameters induces homoclinic bifurcations that change the structure of the trellis. Increasing the detuning ω from 0.278 to 0.282 keeping the injection rate K fixed causes the development of a full Smale horseshoe in R; see Ref. [3] for details.

We finish with an example of a *boundary crisis*[4] in which a chaotic attractor is destroyed. The laser exhibits chaotic dynamics for $K = 0.280$ and $\omega = 0.267$; see Figure 3(a). Increasing the detuning ω results in the destruction of the chaotic attractor in a homoclinic tangency at $\omega \approx 0.2693$; see Figure 3(b). After this bifurcation the system settles on a limit cycle; see Figure 3(c). The ω-limit set of the lower branch of the unstable manifold is shown in grey in Figure 3. After the bifurcation it extends beyond the stable manifold of the saddle (and goes to a periodic orbit not shown in the figure), which is the hallmark of a boundary crisis. We remark that although the *observed* behaviour of the system becomes simpler, the topological entropy bound increases through this bifurcation.

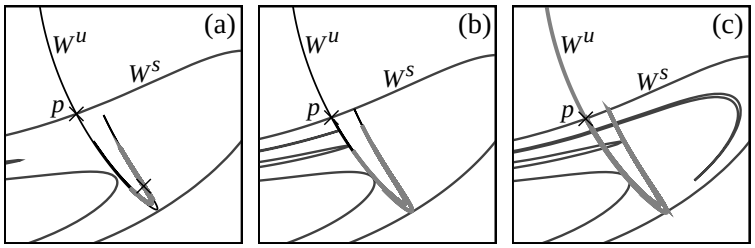

Figure 3. (Un)stable manifolds before (a) , at (b), and after (c) the destruction of a chaotic attractor in a boundary crisis; from (a)–(c) $K = 0.280$ and $\omega = 0.267$, $\omega = 0.2693$, and $\omega = 0.270$, respectively.

3. Conclusions

We have shown that the semiconductor laser exhibits chaotic dynamics by computing symbolic dynamics and a lower bound for the topological entropy of the return map. Directions for further study include a systematic analysis of the possible bifurcations of discontinuous return maps, and the continuation of homoclinic tangencies to find the underlying bifurcation diagram.

References

1. Mladen Bestvina and Michael Handel. Train-tracks for surface homeomorphisms. *Topology*, 34(1):109–140, 1995.
2. Pieter Collins. Dynamics of surface diffeomorphisms relative to homoclinic and heteroclinic orbits. Preprint.
3. Pieter Collins and Bernd Krauskopf. Entropy and bifurcations in a chaotic laser *Phys. Rev. E* 66(5):056201, 2002.
4. Celso Grebogi, Edward Ott, and James A. Yorke. Crises, sudden changes in chaotic attractors, and transient chaos. *Phys. D*, 7(1-3):181–200, 1983.
5. Bernd Krauskopf and Hinke Osinga. Two-dimensional global manifolds of vector fields. *CHAOS*, 9(3):768-774, 1999.
6. Leonid P. Shilnikov, Andrey L. Shilnikov, Dmitry Turaev, and Leon O. Chua. *Methods of qualitative theory in nonlinear dynamics. Part II.* World Scientific Series on Nonlinear Science, Series A, Vol. 5. World Scientific Publishing, River Edge, NJ, 2001.
7. Sebastian M. Wieczorek, Bernd Krauskopf, and Daan Lenstra. A unifying view of bifurcations in a semiconductor laser subject to optical injection. *Opt. Comm.*, 172(1-6):279–295, 1999.
8. Xiao-Song Yang, Senlin Xu, Jiaqiang Mei, and Yilong Ni. Topological obstruction to existence of global poincaré section. *Math. Appl.*, 12(2):72–75, 1999.